A&A manuscript no.
(will be inserted by hand later)

Your thesaurus codes are:
02.04.2 - 03.13.4 - 06.15.1 - 06.16.1

ASTRONOMY AND ASTROPHYSICS
22.5.1997

Diffusion near solar core

P. Morel[1,3] **and E. Schatzman**[2,3]

[1] Département Cassini, URA CNRS 1362, Observatoire de la Côte d'Azur, BP 229, 06304 Nice CEDEX 4, France
[2] DASGAL, URA CNRS 335, Observatoire de Paris, 92195 Meudon Principal CEDEX, France.
[3] GDR, CNRS G131, Observatoire de Paris, 92195 Meudon Principal CEDEX, France.

Received date; accepted date

Abstract. Qualitative reasoning leads to the conclusion that taking into account a proper diffusion process would provide a non-standard solar model (NSSM) giving smaller neutrinos fluxes and being compatible with helioseismology data. The actual theory of the diffusion process is not approached in the present paper. It is just mentioned that a phenomenological representation of the macroscopic diffusion process by a gaussian, having its maximum D_0 (of the order of $10^3\,\mathrm{cm}^2\,\mathrm{s}^{-1}$) at a distance R_0 (of the order of $0.2R_\odot$) of the solar center and a half-width $R_\odot\sigma$ (of the order of $0.04R_\odot$) is acceptable. This phenomenological representation can be improved including in the complete description the microscopic diffusion coefficient. The present numerical experiment appears to show that it is, possible to decrease appreciably the difference between observational data and NSSM.

Key words: Diffusion - Methods : numerical - Sun : oscillations - Sun : particule emission

1. Introduction

The origin of the solar neutrinos fluxes deficiency is considered presently as being due, either to neutrino properties (Anselmann *et al.*, 1992, 1994), or to departures from Standard Solar Models. We consider here the effect of macroscopic diffusion with a phenomenological model inspired by the model of Schatzman (1993) and Schatzman & Montalban (1995).

1.1. Data related to the physics of the central region of the Sun

The physical conditions present in these regions are responsible of the solar neutrinos fluxes and of the important quantity derived from helioseismology data $\delta\nu_{0,2}$: the average value of the frequency difference between two radial p-modes of low degree $l = 0$ and $l = 2$, measured in several orders, $\delta\nu_{0,2} = 9.27 \pm 0.07\mu$Hz (Toutain & Frölich, 1992). We have presently three kinds of data concerning solar neutrinos (Davis, 1993; Hirata *et al.*, 1991; Anselmann *et al.*, 1994) :

- Chlorine experiment, detecting neutrinos of energy $W_{\rm Cl} > 0.7$Mev and giving a flux $\Phi_{\rm Cl} = 2.28 \pm 0.23$ SNU;
- Gallium experiment, detecting neutrinos of energy $W_{\rm Ga} > 0.25$Mev and giving a flux $\Phi_{\rm Ga} = 79 \pm 12$ SNU;
- Kamiokande experiment, detecting neutrinos of energy $W_{\rm K} > 7$Mev and giving a flux $\Phi_{\rm Kam} = 0.28 \pm 0.03$ ev/d.

Altogether, we have four quantities and, assuming massless neutrinos, any attempt to bring the theoretical neutrinos fluxes to the observed values must save the fit between the theoretical and the measured $\delta\nu_{0,2}$; this last quantity, having a small error bar, is the most reliable.

Concerning the interpretation of the neutrino deficiency, it is necessary to decide what has to be compared to what. The chlorine experiment provides now the solar neutrinos fluxes over a period of almost thirty years, whereas GALLEX and SAGE experiments (which are two versions of similar experiments using Ga as a target) and Kamiokande measurements are more recent. Should we compare the averages fluxes $< \Phi_{\rm Cl} >$, $< \Phi_{\rm Ga} >$, $< \Phi_{\rm Kam} >$ over the same period of time, or should we compare the averages taken over the whole duration of each measurements? It is well known (Davis, 1994; Gavryuseva & Gavryusev, 1994) that in the last case, the deficiencies are quite different. This has raised the question of a possible dependance of the solar neutrinos fluxes on variations of the solar physical conditions. This question is presently not settled.

The Mikheyev-Smirnov-Wolfenstein (MSW) mechanism (Anselmann *et al.*, 1992, 1994) has been used to interpret the solar neutrinos fluxes deficiencies : Massive neutrinos, interacting with solar electrons during their propagation inside the Sun can present a resonant rate of oscillations $\nu_e \leftrightarrows \nu_\mu$, between the two neutinos flavors

Send offprint requests to: E. Schatzman, schatzman@obspm.fr

e and μ, which depend on neutrinos energy, electron density and, naturally, on neutrinos properties. The estimate of this effect is based on a Standard Solar Model (SSM), it depends on cross section (Dzitko *et al.*, 1995) and assumes implicitly a steady solar neutrinos production. The result depends on the function of the energy spectrum of the detected neutrinos. It appears possible to fit together the deficiency shown by the three kinds of experiments presently availble; it has nevertheless to be noticed that the fit between the observations and the model of massive neutrinos is marginally acceptable.

There remains the possibility of considering a Non-Standard Solar Model (NSSM) taking into account physical processes of macroscopic diffusion which are ignored in SSM. This is the aim of the present paper.

1.2. Diffusion

The idea that microscopic and macroscopic diffusion processes are present in stars is not a new one. Schatzman (1969) considered how a macroscopic diffusion process would affect gravitational separation of elements, and gave (Schatzman, 1970) an expression of the turbulent diffusion coefficient induced by meridional circulation in good agreement with further estimates (Endal & Sofia, 1978; Zahn, 1983; Pinsonneault *et al.*, 1989). Due to the calibration constraint, it was clear that a diffusion process, bringing ^{3}He to the solar core, would produce a decrease of the central temperature and then leads to a smaller production of high energy neutrinos, due to ^{7}Be and ^{8}B β-decay. It was then very tempting to take into account a macroscopic diffusion process in a model of evolving Sun.

Considering the hydrodynamical model available, it seemed reasonable to assume the presence of turbulent diffusion, with a coefficient $D_{\rm turb} = R_{\rm e}^{*}\nu$, the pseudo-Reynolds number, $R_{\rm e}^{*}$, being supposed to be constant throughout the whole Sun, ν being the turbulent viscosity. It was easy to choose the numerical value of the phenomenological coefficient $R_{\rm e}^{*}$ explaining the solar neutrinos deficiency (Schatzman & Maeder, 1981; Schatzman *et al.*, 1981). It was encouraging to notice that the choice of the diffusion coefficient was leading to a reasonable explanation of the solar lithium deficiency (Schatzman *et al.*, 1981).

However, the new helioseismology data (e.g. Duvall & Harvey, 1984) were quickly shown (Cox & Kidman, 1984; Provost, 1984; Christensen-Dalsgaard, 1986) to be incompatible with the model of strong uniform diffusion of Schatzman *et al.* (1981). Furthermore, lithium deficiency in main sequence stars which, at first look, seemed to be easily explainable by the small macroscopic diffusion process assumed to be present in the Sun (Schatzman *et al.*, 1981), turned out to be relevant of a much more elaborate theory of the diffusion process. As this paper is not the place of a complete review of the lithium problem, let us just mention that the attempts of Charbonnel *et al.* (1992) to describe the time dependance of lithium abundance by a rotation dependent diffusion coefficient, like the one suggested by Zahn (1990), turned out to raise new difficulties when taking into account the real initial distribution function (Bouvier, 1994) of velocities of rotation of stars in galactic clusters (Schatzman, 1994; Schatzman & Montalban, 1995; Montalban, 1995).

1.3. Microscopic diffusion

In the models including microscopic diffusion of ^{4}He and ^{1}H, the computed neutrinos fluxes are larger than in SSM (Michaud & Proffitt, 1991; Chaboyer *et al.*, 1992; Richer & Michaud, 1993). In fact, around the center, the abundance of ^{1}H is depleted by microscopic diffusion, while the abundance of ^{4}He is increased. A direct consequence of this lowering of the available nuclear fuel, is a decrease of the thermonuclear energy production. The calibration process results an increase of the central temperature and a concomitant increase of the neutrinos fluxes. Then microscopic diffusion alone acts in the wrong direction.

1.4. Stochastic gravity waves

The need of taking into account a still ignored physical process (Schatzman & Baglin, 1991) led Schatzman (1991a, 1991b, 1991c, 1993) and Montalban (1994), following a suggestion of Zahn (1990) to consider the effect of stochastic gravity waves. Press (1981) and Press & Ribicky (1981) had given the order of magnitude of the diffusion process induced by gravity waves. From the order of magnitude given by Press (1981), it appeared clearly that diffusion induced by gravity waves was not negligible. Press (1981) considered the possibility of two different processes :

1. The shear due to the large vertical gradient of the horizontal velocity field could generate turbulence. This process has been studied by Garcia-Lopez & Spruit (1991), and seemed to have a limited range of action in spectral type ($M \sim 1.3 - 1.5 M_{\odot}$).
2. The effect of non-adiabatic motion. Bretherton (1969) had shown that adiabatic vertical motion due to gravity waves would not produce any mixing. Contrary to the situation of the adiabatic case, radiative damping would generate second order non-zero mean displacement and non-zero mean velocity. The estimate of the diffusion coefficient by Press (1981) was simply of the order of :

$$D \simeq \left(\frac{k_{\rm V}\, u_{\rm V}}{\omega}\right)^4 \; \frac{D_{\rm th}^2 k_{\rm V}^2}{\omega}, \tag{1}$$

where $k_{\rm V}$ is the vertical wave number, $u_{\rm V}$ the amplitude of the vertical velocity, $D_{\rm th}$ the thermal diffusivity and ω the angular frequency of the wave.

It was obviously necessary to take into account the spectral properties of the gravity waves, supposed to be generated by the turbulent flow at the boundary of the radiative zone. The first attempts (Schatzman, 1993; Montalban, 1994) to take into account the properties of the mechanism generating gravity waves was based on the assumption of the presence of a Kolmogoroff spectrum of the velocity field at the boundary between the radiative and the convective zone. The order of magnitude of the new diffusion coefficient was such that it led to a consistent (non-rotation dependent) model of lithium deficiency. However, the fact that the choice of the phenomenological parameters had something arbitrary was unsatisfactory.

It appeared better to use a model based on the treatment of stochastic differential equations (Knobloch, 1977). It involves a description of the auto-correlation properties of the stochastic motion generating gravity waves. In this respect, plume model of the motion in the convective zone (Rieutord & Zahn, 1995) leads to a description with little dependance of phenomenological parameters. Applications to lithium abundance problems (Schatzman & Montalban, 1995) are quite satisfactory and show, at least, that diffusion due to stochastic gravity waves cannot be ignored even if, in the present situation, rotation has not been taken into account.

1.5. Diffusion near central core

Gravity waves propagate down to stellar center. The diffusion coefficient (Schatzman, 1995) presents first a fast decrease, due to radiative damping; when approaching stellar center, convergence of the waves produces a divergence of the diffusion coefficient like R^{-12}. Near the center, due to the presence of a gradient $\nabla\mu$, of the mean molecular weight μ, diffusion process has to work against gravity. The total flux of mechanical energy decreases, and the diffusion coefficient vanishes like R^2 when R goes to zero. The result is that the diffusion coefficient presents a maximum at some distance R_0 to the center of the Sun of the order of $\sim 0.2R_\odot \sim 0.3R_\odot$.

The theory of the diffusion process induced by stochastic gravity waves is still in a preliminary state and provides only indications of the magnitude and shape of the macroscopic diffusion coefficient curve. We present here a numerical experiment of a NSSM, with the representation by a gaussian, Eq. (3), of the macroscopic diffusion coefficient. It is possible to include in the numerical treatment the contribution of microscopic diffusion process, which can smooth the shape of the curve of the sound velocity $c(R)$, which plays an important role in the determination of $\delta\nu_{0,2}$. Section 2 describes the basis of the numerical experiment; the physics used in the models is shortly described in section 3 with a fast mention of the numerical procedure for which more details can be found in Appendix A. Section 4 is devoted to a presentation of the results, to their analysis and to the discussion; conclusions are given in section 5.

2. Diffusion model

2.1. Presentation of the model

As we have seen, the diffusion coefficient due to Stochastic Internal Waves (SIW) presents a maximum at some distance from the center. This appears exactly as the kind of physical process which could explain the neutrinos deficiency and be consistent with helioseismology data. Let us first discuss qualitatively the effect of such a diffusion coefficient.

Due to the ^{3}He gradient, diffusion drags ^{3}He towards the solar center and increases the rate of the most energetic reaction of the PPI cycle, ^{3}He(^{3}He,2p)^{4}He. Consequently, the calibration of the solar model leads to a decrease of the central temperature. The contribution of the PPI reactions becomes a larger fraction of the energy production. Altogether, it results in a decrease of the central concentration of ^{4}He and a fall of the central temperature which leads to a smaller rate of neutrinos production.

Due to the fact that the diffusion coefficient becomes very small near the solar center, the general shape of the function $\mu(R)$ remains similar to the same function of SSM. The consequence, for helioseismology, can easily be seen on the expression of the asymptotic quantity A (Turck-Chièze *et al.*, 1993) :

$$A = \frac{1}{4\pi^2}\left[\frac{c\,(R_\odot)}{R_\odot} - \int_0^{R_\odot}\frac{1}{R}\frac{dc}{dR}\,dR\right] \qquad (2)$$

where c is the velocity of sound. For the modes of low degree l the frequency difference writes :

$$\delta\nu_{l,l+2}(n) \equiv \nu_{n+1,l} - \nu_{n,l+2} \sim \frac{2(2l+3)A}{n+l/2+\varepsilon} \equiv 2(2l+3)\mathcal{D}_l$$

n is the radial order of the mode, ε depends on the reflecting properties of the surface; for $l \equiv 0$, the observed quantity, $\mathcal{D}_0 = 1.52\mu$Hz, leads to a constraint on the derivative of sound speed near the center through the quantity A. The decrease of the sound velocity, when approaching the very central regions remains an important property, as it keeps there a negative contribution to the integrand in the quantity A given by Eq. (2).

However the asymptotic quantity A ignores the effects of the variations of N^2, the Brunt Väissälä frequency. The meaning of the exact value of the frequency difference $\delta\nu_{0,2}$, which has to be compared with the observed value, is given in section 4.1.

Formally, it is also necessary to take into account the effect of diffusion on ^{7}Li and ^{7}Be. However, as the time scale of nuclear reactions is much shorter than the time scale of the diffusion processes, the concentrations of ^{7}Li and ^{7}Be remain close to their local balance concentrations.

We have made the choice of a time independent macroscopic diffusion coefficient. It should be noticed that this is really an oversimplification. The propagation of gravity waves, as well as the work against gravity are $\nabla\mu$ dependent. $\nabla\mu$ is, obviously, time dependent and then the correct model should include the complete model of the diffusion coefficient. But, as it has been said in the introduction, the theory of the diffusion coefficient is still in a preliminary state, and the above mentioned oversimplification can be considered as a step towards the solution of the problem.

2.2. Choice of the diffusion coefficient

In the calculations the diffusion coefficient $D_{\rm SIW}(R)$ is mimicked by a gaussian shaped function of the radius R centered at $R = R_0$, with high D_0 and given by :

$$D_{\rm SIW}(R) = D_0 \exp\left(-\frac{1}{2}\left(\frac{R-R_0}{R_\odot\sigma(R)}\right)^2\right), \tag{3}$$

σ is the asymmetric half-width of the gaussian taken as :

$$\sigma(R) = \begin{cases}\sigma_{\rm L} & \text{if } R \le R_0,\\ \sigma_{\rm R} & \text{otherwise,}\end{cases}$$

with $\sigma_{\rm R} = p\sigma_{\rm L}$ and $p \ge 1$.

2.3. Diffusion of chemical

In the assumption of spherical symmetry, the diffusion equation, in conservative form, can be written when completed by the term $\Psi_i(T,\rho,\mathcal{X})$ coming from nuclear reactions :

$$\frac{\partial X_i}{\partial t} = -\frac{1}{\rho R^2}\frac{\partial F_i}{\partial R} + \Psi_i, \quad 1 \le i \le n_{\rm X}. \tag{4}$$

where the flow, $F_i(R,t)$, of the chemical element X_i writes :

$$F_i = -4\pi R^2 \rho D_i \frac{\partial X_i}{\partial R}, \tag{5}$$

$n_{\rm X}$ is the total number of chemical species, ρ is the density, T the temperature, $\mathcal{X} \equiv {}^T(X_1,\dots,X_{n_{\rm X}})$ is the vector of chemical abundances and $D_i(R)$ is the coefficient of diffusion for the chemical specie indexed by i. Microscopic diffusion, which acts against the lowering of the neutrinos fluxes, has been ignored, then we have : $D_i(R) \equiv D_{\rm SIW}(R)$

Boundary conditions : It is assumed that there is neither input nor output of matter neither at the center nor at the surface of the solar model :

$$F_i(0,t) = 0,\ F_i(R_{\rm ext}(t),t) = 0,\ i = 1,\dots,n_{\rm X}, \tag{6}$$

with $R_{\rm ext}(t)$ as the radius of the solar model at time t.

2.3.1. Choices of the parameters

We obviously meet here a phenomenological question. Near the maximum of the diffusion coefficient $D_{\rm SIW}$, it is estimated to use a representation by a Gaussian Eq. (3). In fact, it turns out that, with the mathematical properties given above, in the range $0.01D_0$ to D_0 of $D_{\rm SIW}$, the diffusion coefficient is very close to be gaussian. As long as we do not have a complete consistent theory of $D_{\rm SIW}$, the choice is defined by the properties described at the beginning of section 1.5 :

1. In order to keep the change of sign of $\frac{dc}{dR}$ in Eq. (2), the position of R_0 of the maximum should not be too close of the center in order to avoid too much mixing in the region of maximum rate of thermonuclear reactions, as it does with the pseudo-Reynolds number $R_{\rm e}^*$.
2. For the same reason the width of the gaussian should not be too large.
3. The maximum D_0 of $D_{\rm SIW}$ remains an arbitrary phenomenological parameter.

With : $10^2{\rm cm}^2\ {\rm sec}^{-1} < D_0 < 10^5{\rm cm}^2\ {\rm sec}^{-1}$, $0.1R_\odot < R_0 < 0.3R_\odot$, $0.02 < \sigma_L < 0.05$ and $.02 < \sigma_R < 0.12$ it is possible to carry the numerical experiment which can tell us if it is worth having a better approach of the diffusion coefficient $D_{\rm SIW}$.

2.4. Mixing in the convective zones

As seen from numerical simulations (Hurlburt *et al.*, 1986; Steffen & Freytag, 1991; Cattaneo & Malagoli, 1992; Steffen, 1993) a Convective Zone (CZ) is the seat of large scale motions. The Reynolds number, $R_{\rm e} = (lv/\nu)$ (ν is the microscopic viscosity, l and v are characteristic magnitudes of the size of the system and of the velocities), is very large and we can assume the presence of a large turbulent diffusion process. The correspondent turbulent diffusion coefficient $D_{\rm T}$ is certainly not isotropic. The vertical diffusion coefficient, of the order of $\mathcal{L}\mathcal{V}$ ($\mathcal{L}$ is of the order of the pressure scale height and $\mathcal{V}$ is any of the estimates of the vertical turbulent velocity), turns out to be of the order of $D_{\rm T} \sim 10^{12}\,{\rm cm}^2\,{\rm s}^{-1} \sim 10^{13}\,{\rm cm}^2\,{\rm s}^{-1}$.

In any CZ of the model, the characteristic time scale of convection is small with respect to thermonuclear time scales. Therefore the CZ are *quasi-instantaneously* homogenized and there the flow in Eq. (5) then write :

$$F_i = -4\pi R^2 \rho D_{\rm T} \frac{\partial X_i}{\partial R}. \tag{7}$$

In this paper $D_{\rm T} \equiv 10^{13}\ {\rm cm}^2{\rm sec}^{-1}$ is used. It corresponds to a characteristic time scale for the mixing of the solar CZ of about one year and it is of the same order of magnitude for the convective core of the young Sun. That is very small compared to the nuclear reactions time scale which is million times greater. Therefore, in RZ the diffusion coefficient remains $D_i \equiv D_{\rm SIW}$ while, in CZ it becomes

$D_i = D_T$ for all the chemical species. Note that a consequence of the mixing, is a discontinuity of the diffusion coefficient at each limit of any CZ.

Due to diffusion, the chemical abundances X_i are continuous functions and, as a consequence of mixing, their first derivatives are discontinuous at the boundaries of the CZ. Indeed, as a result of the conservation of matter, since $D_{\rm T} \sim \infty$, the flow F_i are continuous functions and their first derivatives $\frac{\partial F_i}{\partial R}$ are discontinuous at the boundaries of the CZ.

3. Global characteristics of solar models

We have computed the evolution of NSSM including diffusion with SIW, starting from the chemically homogeneous Zero Age Main Sequence model (ZAMS) to the present solar age, here assumed to be 4.55Gy. The solar models are calibrated by adjusting the mixing-length parameter and the initial mass fraction Y of helium in order to have, at present day, the luminosity equal to $L_\odot = 3.846\,10^{33}$erg sec^{-1} and, for the radius $R_\odot = 6.9599\,10^{10}$cm. The mass of the Sun is taken as $M_\odot = 1.989\,10^{33}$ g. For consistency of the comparisons, the SSM reference model is computed as a NSSM with SIW diffusion $D_{\rm SIW} \equiv 0$ in RZ and, in CZ, turbulent diffusion $D_{\rm T} = 10^{13}$ cm^{2}sec^{-1}. Moreover, for this phenomenological study of the diffusion near the solar core, we have used standard physics and physical data, therefore the SSM model slightly differs from the SSM of Berthomieu *et al.* (1993) which is computed, with the same code, but with more sophisticated data. We estimate that improvements of physics and of the numerical accuracy can change the results of the present calculations within $\sim \pm 5\%$.

We have used the OPAL opacity data of Rogers & Iglesias (1992) extended with the low temperature opacities of Kurucz's (1991) with an abundance, in mass, for the heavier elements fixed to $Z = 0.0194$. The basic formulation, according to Henyey *et al.* (1965), of the classical mixing length theory is used. At the surface, the outer boundary conditions are written through a simplified atmosphere of only one shell with a Rosseland optical thickness $\tau_{\rm R} \equiv 1$. Neither overshooting nor convective penetration have been introduced. The EFF equation of state (Eggleton *et al.*, 1973) is used. The general nuclear network contains the following 12 species which enter into the most important nuclear reactions of the PP and CNO cycles (Clayton, 1968) : ^{1}H, ^{2}D, ^{3}He, ^{4}He, ^{7}Li, ^{7}Be, ^{12}C, ^{13}C, ^{14}N, ^{15}N, ^{16}O, ^{17}O. Most of the models are computed assuming ^{2}D, ^{7}Li and ^{7}Be at equilibrium. The relevant nuclear reactions rate are taken from the tabulations of Caughlan and Fowler (1988). Weak screening is assumed. The initial abundances are the meteoritic abundances of Anders & Grevesse (1989). The rate of neutrinos losses are computed according to Berthomieu *et al.* (1993).

3.1. Numerical procedure

The solar models discussed in this paper have been computed with the code CESAM (Morel, 1989, 1993). New algorithms (Morel, 1995) have been implemented for the numerical integration of the diffusion equation. They are outlined in Appendix A. For this phenomenological study, the models were computed with a modest numerical accuracy using 200 shells, a fourth order scheme for the internal structure and a first order scheme for the diffusion equation. The four models of Table 1, SSM, 20 231, 20 331 and 20 441, were also computed with 300 shells, a fourth order scheme for the internal structure and a second order scheme for the diffusion; no significant change on the global characteristics of the models was observed.

4. Results and discussion

4.1. The solar models

In Table 1 the observations, the global characteristics of SSM and of NSSM computed with $R_{\rm e}^*$ and SIW diffusion coefficient are reported. R_0, $\sigma_{\rm L}$, D_0 and p are the parameters of the gaussian of Eq. (3); $\Phi_{\rm Ga}$, $\Phi_{\rm Cl}$, $\Phi_{\rm Kam}$ are the predicted neutrinos fluxes for the three experiments; A is the asymptotic helioseismological quantity computed by Eq. (2); Y is the initial abundance in ^{4}He; $X_{\rm c}$, $T_{\rm c}$ and $\rho_{\rm c}$ are the values, at the center, of respectively ^{1}H abundance, temperature and density. The frequencies difference, $\delta\nu_{0,2}$ is computed in a way coherent with the observations via a polynomial fit around the radial order $n_0 = 21$ according to the procedure detailed in Berthomieu *et al.* (1993) section 3.3.2.

4.2. General properties

With respect to SSM, with the chosen shape of the diffusion coefficient, the presence of diffusion brings down, as expected, the solar neutrinos fluxes, either $\Phi_{\rm Cl}$, $\Phi_{\rm Ga}$ or $\Phi_{\rm Kam}$.

As in SSM, the velocity of sound shows, in any case, a maximum located at about the same distance from the center. Another effect of diffusion is also to decrease the mean molecular weight but, as $D_{\rm SIW}$ vanishes in the very central region, the mean molecular weight is practically unchanged. Figure 1 and Fig. 2 give examples of these properties. The consequence is that the negative contribution to the integral A given by Eq. (2) is increased, therefore A reaches smaller values than in SSM.

As noticed in the introduction, the first model with diffusion (Schatzman *et al.*, 1981) led to results incompatible with helioseismology data. As convincingly shown in Fig. 1, for the model labelled by $D_{\rm R^*}$, there was no negative contribution to the integral A , leading to an unacceptable high values of $\delta\nu_{0,2}$. Further attempts (Lebreton & Maeder, 1987), with a diffusion coefficient having a maximum at the center were also leading to results incompatible with helioseismology. What appear here, is that there is the possibility to improve the situation by introducing a little more mixing in the very central regions. That can be done by a process such as the microscopic diffusion. Solar models including both, SIW diffusion and microscopic diffusion according to Michaud & Proffitt, (1991), have been calculated. They exhibit a slight increase of the neutrinos fluxes and no change for the frequency difference $\delta\nu_{0,2}$. These results are not detailed here.

4.3. Position of the maximum $D_{\rm SIW}$ of the gaussian

For the *fixed* value $\sigma = 0.04$, we have plotted, Fig. 3 right, the values of the neutrinos fluxes $\Phi_{\rm Cl}$, $\Phi_{\rm Ga}$ and $\Phi_{\rm Kam}$ and the helioseismologic quantity $\delta\nu_{0,2}$ as functions of the normalized position of the maximum $R_0/R_\odot$. The closer to the center the localization of the maximum of $D_{\rm SIW}$ is, the higher will be the decrease of the neutrinos fluxes. On the other hand, the behaviors of A and $\delta\nu_{0,2}$ with respect to R_0 is not clearly intelligible : the integral A is smaller while $\delta\nu_{0,2}$ is higher. It is known (Provost, 1995) that the asymptotic representation of A of Eq. (2), does not give always the correct eigen value of $\delta\nu_{0,2}$. Notice especially that negative values of A (see models 15 431, 20 451 and 20 541 of Table 1) do not correspond to negative values of $\delta\nu_{0,2}$.

As noticed by Provost (1995), the sharp decrease of the diffusion coefficient on both sides of its maximum, produces large anomalies of $\nabla\mu$ and then, of the sound velocity (Fig. 2) and then also of N^2. The too large values of $\delta\nu_{0,2}$ are probably due to these large gradients of N^2.

4.4. Width, amplitude and asymmetry of the gaussian $D_{\rm SIW}$

This is the most interesting aspect of the results of this numerical experiment. For the *fixed* value $R_0 = 0.2R_\odot$ of the position of the maximum, we have plotted, Fig. 3 left, the previous quantities for different values of the amplitude $D_{\rm SIW}(R_0) = 10^3\,{\rm cm^2\,s^{-1}}$, $10^4\,{\rm cm^2\,s^{-1}}$ and $10^5\,{\rm cm^2\,s^{-1}}$, as functions of widths σ of the gaussian. When increasing the width σ, or increasing the amplitude D_0, we obtain smaller values of the neutrinos fluxes. This is the expected result. We meet again the expected decrease of the integral A, and the unexpected increase of $\delta\nu_{0,2}$. The frequency difference $\delta\nu_{0,2}$ is not so sensitive than A to the negative contribution of $\frac{1}{R}\frac{dc}{dR}$.

An asymmetric profile of the $D_{\rm SIW}$ allows an extended drag towards regions reacher in ^{3}He; as seen for the models 20 342, 20 343 and 20 344 the effect of this asymmetry on the neutrinos fluxes remains small.

5. Conclusion

Diffusion due to SIW assumes transport of ^{3}He to the central regions. Due to the calibration, this increase in

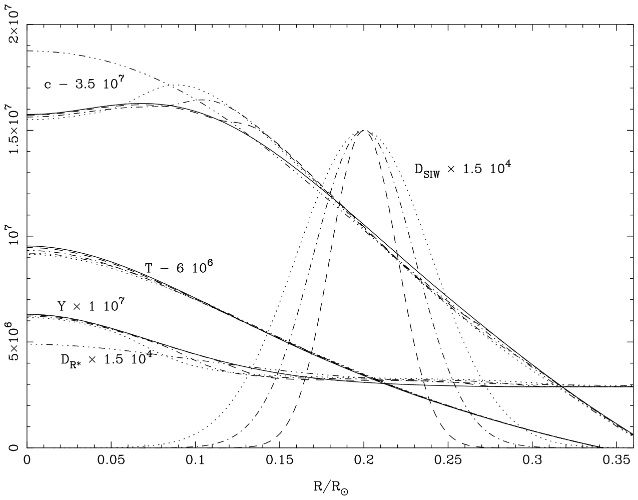

Fig. 1. The sound velocity (c), the temperature (T) and the ^{4}He (Y) profiles are plotted for the NSSM models $R_{\rm e}^*$, 20 231, 20 331 and 20 431 of Table 1 and, in full line, for the Standard Solar Model. The diffusion coefficients are either, gaussian shaped functions $D_{\rm SIW}$ centered at R=$0.2R_\odot$, of high $D_0 = 10^3$ cm^2 sec^{-1}, with half-widths $\sigma = 0.02$ (dash), 0.03 (dash dot dash), 0.04 (dot) or, $D_{\rm R^*}$ (dash dot dot dot dash), calculated with the pseudo-Reynolds number $R_{\rm e}^* = 75$. As far as the diffusion coefficient is enlarged, the central temperature is depressed leading to lower neutrinos fluxes.

^{3}He concentration brings down the central temperature and the neutrinos fluxes.

We can consider that with, around the center, a phenomenological diffusion coefficient of gaussian shape, with a maximum located at some distance of the center (*e.g.* $R_0 = 0.2R_\odot$), with a moderate width ($\sigma = 0.04$) and a relatively large value of $D_{\rm SIW}$, $D_{\rm SIW}(R = R_0) = 10^4$ cm^2 sec^{-1} it is possible to obtain an appreciable decrease of the neutrinos fluxes. However the impossibility of reducing appreciably ^{7}Be neutrino flux keeps the flux in gallium experiment too high.

Then remains the question of improving the agreement with seismology data. The prospect seems to smooth a little the diffusion coefficient in the very central part of the core. The effect would be to bring a little more ^{3}He to the center, and also to smooth the function $\mu(R)$ this is likely to reduce the anomalies of N^2. We know from the first approach of the solar neutrino problem (Schatzman *et al.*, 1981) that too much mixing near the center produces a large increase of the integral in A. But we are here in the

Table 1. Global characteristics of Non Standard Solar Model with Stochastic Internal Wawe diffusion coefficient of gaussian shape.

model	R_0	σ_L	D_0	p	Φ_{Ga}	Φ_{Cl}	Φ_{Kam}	A	$\delta\nu_{02}$	Y	X_c	T_c	ρ_c
	$R_\odot$		cm^2 s^{-1}		SNU	SNU	ev/d	μHz	μHz			10^7K	g cm^{-3}
observed					79	2.28	.28		9.3				
SSM					119	6.68	.52	39.0	9.3	.288	.35	1.554	150
$Re^* = 75$					107	3.18	.34	63.5	14.9	.291	.49	1.520	117
15 231	.15	.02	10^3	1.	110	4.87	.36	36.9	11.2	.289	.36	1.525	145
15 331	.15	.03	10^3	1.	105	4.01	.29	30.2	12.3	.291	.37	1.504	137
15 431	.15	.04	10^3	1.	102	3.62	.26	-6.0	13.7	.293	.38	1.496	128
15 441	.15	.04	10^4	1.	97	2.77	.19	42.2	13.8	.296	.56	1.480	102
15 451	.15	.04	10^5	1.	96	2.73	.18	71.9	14.2	.300	.61	1.475	94
18 431	.18	.04	10^3	1.	104	3.84	.27	30.1	11.8	.292	.37	1.501	137
18 441	.18	.04	10^4	1.	97	2.74	.18	-17.8	13.5	.296	.39	1.474	123
18 451	.18	.04	10^5	1.	95	2.52	.17	22.1	14.1	.300	.55	1.470	100
19 441	.19	.04	10^4	1.	98	2.81	.19	14.9	13.2	.296	.38	1.474	126
19 541	.19	.05	10^4	1.	95	2.51	.17	27.3	13.7	.298	.53	1.471	104
19 551	.19	.05	10^5	1.	94	2.40	.16	69.7	14.1	.301	.62	1.468	93
20 231	.20	.02	10^3	1.	117	6.12	.47	38.9	9.0	.289	.35	1.546	149
20 241	.20	.02	10^4	1.	114	5.51	.42	38.7	9.1	.290	.35	1.537	146
20 251	.20	.02	10^5	1.	110	4.85	.36	38.4	9.5	.291	.36	1.527	145
20 331	.20	.03	10^3	1.	112	5.20	.39	38.1	9.6	.290	.36	1.532	147
20 341	.20	.03	10^4	1.	101	3.42	.24	36.8	10.8	.292	.36	1.496	139
20 342	.20	.03	10^4	2.	104	3.64	.25	35.6	10.8	.293	.37	1.501	140
20 343	.20	.03	10^4	3.	104	3.57	.25	35.4	10.7	.294	.37	1.499	140
20 344	.20	.03	10^4	4.	104	3.54	.24	35.3	10.7	.294	.37	1.498	141
20 351	.20	.03	10^5	1.	100	3.07	.21	31.9	12.4	.295	.38	1.483	133
20 431	.20	.04	10^3	1.	107	4.29	.31	35.3	10.7	.291	.36	1.514	142
20 441	.20	.04	10^4	1.	99	2.91	.20	23.5	12.8	.295	.38	1.477	130
20 451	.20	.04	10^5	1.	95	2.49	.16	-43.	13.8	.299	.40	1.466	119
20 531	.20	.05	10^3	1.	104	3.75	.27	25.6	11.7	.292	.36	1.499	136
20 541	.20	.05	10^4	1.	96	2.54	.17	-2.1	13.6	.297	.47	1.471	111
20 551	.20	.05	10^5	1.	94	2.36	.15	63.8	14.1	.300	.61	1.467	94
21 441	.21	.04	10^4	1.	100	3.08	.21	29.2	12.3	.294	.37	1.483	133
21 451	.21	.04	10^5	1.	96	2.53	.17	8.1	13.6	.299	.39	1.465	122
22 431	.22	.04	10^3	1.	111	4.95	.37	37.5	9.8	.290	.36	1.528	146
22 441	.22	.04	10^4	1.	102	3.33	.23	32.6	11.6	.294	.37	1.491	137
22 451	.22	.04	10^5	1.	97	2.61	.17	19.2	13.3	.298	.39	1.467	126
30 441	.30	.04	10^4	1.	117	6.22	.48	38.8	8.9	.289	.35	1.548	150

situation of adding just a little mixing between the center and the maximum of the gaussian.

This phenomenological time independent diffusion coefficient is certainly an oversimplification. We shall conclude by considering the need to introduce a time dependent model of the macroscopic diffusion process.

Acknowledgements. Our thanks to A. Baglin, G. Berthomieu and J. Provost who help us, by their constructive remarks, to write a readable paper.

A. Appendix

A.1. Numerical solution of the diffusion equation

The numerical integration of Eq. (4) is performed with respect to the Lagrangian variable $\zeta \equiv (M/M_\odot)^{\frac{2}{3}}$. That avoids a singularity at the center. The equations to be solved then write :

$$\frac{\partial X_i}{\partial t} = -\frac{2}{3M_\odot\sqrt{\zeta}}\frac{\partial F_i}{\partial \zeta} + \Psi_i, \quad \zeta \in [0,1], \quad 1 \le i \le n_X. \qquad (A1)$$

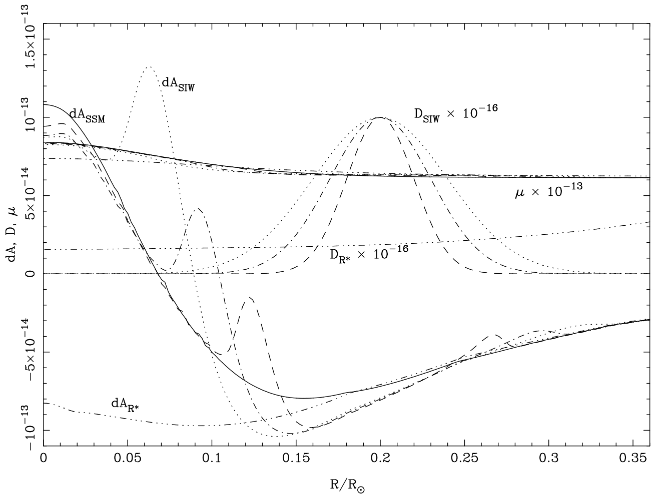

Fig. 2. The same as Fig. 1, for the integrand $dA \equiv \frac{1}{R}\frac{dc}{dR}$ of Eq. (2) and the mean molecular weight (μ). There is a negative contribution to the asymptotic quantity A when $dA(R) > 0$, otherwise the contribution is positive. All models exhibit such a negative contribution to A, except the model computed with the pseudo-Reynolds number $R^*_{\rm e}$. For this model the mean molecular weight is depressed in the vicinity of the center, it is the consequence of a large amount of diffusion there.

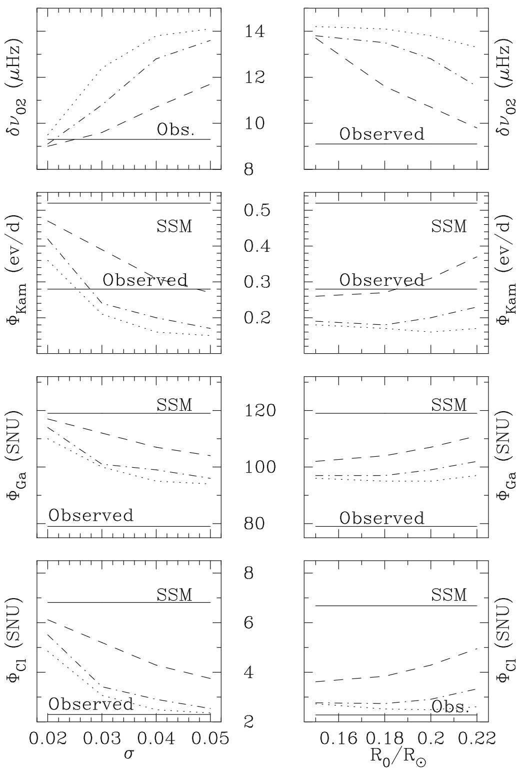

Fig. 3. Left : for the location $R_0 = 0.2R_\odot$ of the maximum $D_0 = 10^3\,{\rm cm}^2\,{\rm s}^{-1}$ (dash), $10^4\,{\rm cm}^2\,{\rm s}^{-1}$ (dash dot), $10^5\,{\rm cm}^2\,{\rm s}^{-1}$ (dot), the predicted neutrinos fluxes and the frequencies difference $\delta\nu_{0,2}$ are plotted as a function of to σ, the width of the diffusion coefficient $D_{\rm SIW}$.
Right : for $\sigma = .04$ the same quantities are plotted as a function of $R_0/R_\odot$. The values observed (Obs.) and/or predicted (SSM) also appear. When increasing the width, or the amplitude of $D_{\rm SIW}$, smaller values for the neutrinos fluxes are obtained.

As seen Sect. 2.4, the mixing in CZ is made by turbulent diffusion. Since Eq. (A1) holds everywhere, the evolution of the chemical composition is a parabolic differential problem with the boundary conditions given by Eq. (6).

For the numerical solution, one seeks the X_i as piecewise polynomials of order s with discontinuous first derivative at each limit of the CZ. For the calculations it is convenient to project the piecewise polynomials on their B-spline basis $\mathcal{B} \equiv \{N^s_k\}_{k=1,K_{\rm X}}$ (de Boor, 1978; Schumaker, 1981). Therefore $X_i(\zeta, t)$ writes :

$$X_i(\zeta,t) = \sum_{k=1}^{K_{\rm X}} x_{i,k}(t) N^s_j(\zeta), \tag{A2}$$

where $N^s_j(\zeta)$ is the value of the j-th normalized B-spline of order s at ζ, the $x_{i,k}(t)$ are the projections, at time t, of the abundance of each specie i on the B-spline $N^s_j(\zeta)$ and $K_{\rm X}$ is the dimension of the basis. The Eq. (A1) are solved for the unknowns $x_{i,k}(t)$. One looks for the *weak solutions* using the Petrov-Galerkin's formalism (Marchouk & Agochkov, 1985; Quarteroni & Valli, 1994); multiplying both sides of Eq. (A1) with N^s_j, $j = 1, \ldots, K_{\rm X}$ and integrating over the whole star :

$$< \frac{3}{2} M_\odot \sqrt{\zeta} \left(\frac{\partial X_i}{\partial t} - \Psi_i \right), N^s_j > + < \frac{\partial F_i}{\partial \zeta}, N^s_j > = 0, \tag{A3}$$

here $< f, g > \equiv \int_0^1 f(\zeta) g(\zeta) {\rm d}\zeta$ is the inner product of the two functions f and g.
The standard integration by parts gives :

$$< \frac{\partial F_i}{\partial \zeta}, N^s_j > = \Big[F_i N^s_j \Big]_0^1 - < F_i, \frac{\partial N^s_j}{\partial \zeta} > . \tag{A4}$$

Owing to the fact that $F_i \equiv 0$ at the boundaries, Eq. (A3), is discretized as :

$$< \tfrac{3}{2} M_\odot \sqrt{\zeta} \Big(X_i - X_i^{(t)} - \Psi_i \Delta t \Big), N^s_j > + \\ + < \tfrac{64\pi^2 R^4 \rho^2 \Delta t}{3\sqrt{\zeta}} D_i \tfrac{\partial X_i}{\partial \zeta}, \tfrac{\partial N^s_j}{\partial \zeta} > = 0 \tag{A5}$$

here all the quantities are taken at the time $t + \Delta t$ except $X_i^{(t)}$ taken at time t; Δt is the time step. The accuracy of this nolinear fully implicit scheme for the unknowns $x_{i,k}(t + \Delta t)$ is of order $s - 1$ in space and first order in time. The system of the non-linear equations (A5) is solved by Newton-Raphson iterations. Since the B-spline basis is a local basis, the jacobian is a $2s - 1$ banded matrix. The inner products are computed by gaussian integration formula with s points on intervals where the integrants are continuous functions. Therefore the limiting values of Eq. (A5) at $\zeta = 0$ are implicitly taken into account. We emphasize on the following four facts : (i) the discontinuities of the first derivatives of the X_i are implicitly taken into account, (ii) the use of the B-spline basis is convenient because the algorithms are simple even if the locations of the limits of the CZ move with time, (iii) the first order derivatives are only involved in the numerical solution of the parabolic diffusion equation, iv) with the use of a B-spline basis, only one algorithm is needed for all s *i.e.* for all orders of numerical accuracy. (Most of the models of Table 1 are calculated with $s = 2$.)

A.2. Calculations with B-splines

Computation with B-splines is not familiar in star modelling, so one briefly describes the basis of the method directed towards the numerical integration of Eq. (4) with discontinuous diffusion coefficient. For more advanced description and proofs refers to de Boor (1978), Shumaker (1981) and to the literature cited herein.

With this technique the functions are approximated by piecewise polynomials. Among all the basis available for the linear set of piecewise polynomials, the B-spline basis, leads to stable algorithms; it is a local basis. A B-spline is itself a piecewise polynomial it is a divided differences of the truncated power function (de Boor, *loc. cit.*, definition IX.1).

A.2.1. The nodal vector : the key of the computations with B-splines

A piecewise polynomial $\mathcal{P}(\zeta)$, of order s, on a given partition Δ of $[\zeta_1, \zeta_n]$, $\Delta \equiv \{\zeta_1 < \zeta_2 < \ldots < \zeta_{n-1} < \zeta_n\}$, is defined as a function which coincides, on each sub-interval $[\zeta_i, \zeta_{i+1}]$, $1 \leq i < n$, with a polynomial of degree $s-1$. The existence and uniqueness of $\mathcal{P}(\zeta)$ on Δ results from the knowledge, at each breakpoint ζ_i, of the kind of connection which is required between the right and the left pieces of polynomials. For each ζ_i, the connection is characterized by m_i, the so-called multiplicity, obtained as follow : let $d_i < s$, $1 < i < n$ be the order of the oscularity of the connection between the left and right polynomial pieces at the breakpoint ζ_i; $d_i = 0$ means $\mathcal{C}^0$ continuity of $\mathcal{P}(\zeta)$ at $\zeta = \zeta_i$, $d_i = 1$ means $\mathcal{C}^1$ continuity *i.e.* continuity of the first derivative of $\mathcal{P}$ at $\zeta = \zeta_i$, $d_i = 2$, means $\mathcal{C}^2$ continuity *etc...* and one sets $d_i = -1$ for a $\mathcal{C}^{-1}$, *i.e.* discontinuity of the function itself at $\zeta = \zeta_i$. At $i = 1$ and $i = n$ (inner and outer boundaries) one fixes the value of $\mathcal{P}(\zeta_i)$; this is equivalent to assume that $\mathcal{P}$ is discontinuous at these points. Hence, one has $d_1 = d_n = -1$. The multiplicity of the point ζ_i is then defined as :

$$m_i \equiv s - (d_i + 1)$$

From the vector of multiplicities : $\mathcal{M} = {}^T(m_1, \ldots, m_n)$ one constructs the heart of the calculation with B-spline : the so-called "nodal vector" : $\mathcal{N}(\Delta,\ \mathcal{M},\ s)$ associated to a B-spline basis. It is the vector which has for coordinates the ζ_i, each of them appearing m_i times. $\mathcal{N}$ schematically writes :

$$\begin{aligned}\mathcal{N} &= {}^T(\overbrace{\zeta_1, \zeta_1, \ldots, \zeta_1}^{m_1}, \overbrace{\zeta_2, \zeta_2, \ldots, \zeta_2}^{m_2}, \ldots, \overbrace{\zeta_n, \zeta_n, \ldots, \zeta_n}^{m_n}) \\ &\equiv {}^T(t_1, t_2, t_3, \ldots, t_{S+m_n}).\end{aligned}$$

The dimension of $\mathcal{N}$ is then $S + m_n$, with $S = \sum_{i=1}^{n-1} m_i$. Once given this nodal vector, the value of the k-th normalized B-spline on $\mathcal{N}$ ($k = 1, 2, \ldots, S$) is obtained by induction, whatever the nodal vector is. Such algorithm is found in Schumaker (1981, algorithm 5-22).

A convenient schematic representation of a nodal vector consists (de Boor, *loc. cit.*) in writing one column of m_i elements for each breakpoint ζ_i. As an example, let a model with $n = 9$ grid points, with a radiative zone between the grid points $i = 1$ and $i = 6$ and a convective zone starting at $i = 6$ and ending at $i = 10$. A schematic representation of the grid is :

$$\begin{array}{cccccccccc} \leftarrow & & RZ & & \rightarrow & \Downarrow & \leftarrow & CZ & & \rightarrow \\ \times & \times & \times & \times & \times & \times & \times & \times & \times & \times \end{array}$$

where the limit of the CZ is symbolized by the arrow $\Downarrow$.

A schematic representation of the nodal vector for the basis $\{N_k^3\}_{k=1}^{k=12}$ with a discontinuous first derivative at the limit of the CZ ($\Downarrow$) at $i = 6$ is :

$$\begin{array}{cccccccccc} \leftarrow & & RZ & & \rightarrow & \Downarrow & \leftarrow & CZ & & \rightarrow \\ \times & \times & \times & \times & \times & \times & \times & \times & \times & \times \\ \times & & & & & \times & & & & \times \\ \times & & & & & & & & & \times \end{array}$$

With this nodal vector the numerical solution to the differential equations will be a parabolic piecewise polynomial with C^1 continuity everywhere except at the limit of the CZ where it is only C^0.

References

Anders, E., Grevesse, N. 1989, Geochimica et Cosmochimica Acta 53, 197

Anselmann, P., Hampel, W., Heusser, G., Kiko, J., Kirsten, T., Pernicka, E., Plaga, R., Rönn, U., Sann, M., Schlossr, C., Wink, R., Wójcik, M., von Ammon, R., Ebert, K.H., Henrich, E., Balata, M., Bellotti, E., Ferrari, N,, Lalla, H., Stolarczyk, T., Cattadori, C., Cremoonesi, O., Fiorini, E., Pezzoni, S., Zanotti, L., von Feilitzsch, F., Mößbauer, R., Schanda, U., Berthomieu, G., Schatzman, E., Carmi, I., Dostrovsky, I., Bacci, C., Belli, P., Bernabei, R., d'Angele, S., Paoluzi, L., Charbit, S., Cribier, M., Dupont, G., Gosset, L., Rich, J., Spiro, M., Tao, C., Vignaud, D., Hahn, R.l., Hartmann, F.X., Rowley, J.K., Stoenner, R.W., Wenesser, J. 1992, Phys. Lett. B 285, 390

Anselman, A., *et al.*, 1994, (GALLEX collaboration), Nucl. Phys. B, Proc. Suppl. 35, 418

Berthomieu, G., Provost, J., Morel, P., Lebreton, Y. 1993, A&A 268, 775

Bouvier J. 1994, The Eight Cambridge Workshop on Cool Stars, Stellar Systems and the Sun, Caillaut J.P. (ed.) (in press)

Bretherton F. P. 1969, J. Fluid Mech. 36, 785

Cattaneo, F. Malagoli, A. 1992, Seventh Workshop on Cool Stars, Stellar Systems and the Sun, Tucson (AZ), Gianpapa M.S. and Bookbinder J.A. (eds.), ASP Conf. Ser., 26, 139

Caughlan, G.R., Fowler, W.A. 1988, Atomic Data and Nuclear Data Tables 40, 284

Chaboyer, B.C., Deliyannis, C.P., Demarque, P., Pinsonneault, M.H., Sarajedini, A. 1992, ApJ 348, 372

Charbonnel, C., Vauclair, S., Zahn, J.P. 1992, A&A 265, 55

Christensen-Dalsgaard, J. 1986, Seismology of the Sun and distant Stars, Proceedings of a NATO Advanced R esearch Workshop, D. O. Gough (ed.), D. Reidel Publishing Company, p. 23
Clayton, D.D. 1968, Principles of Stellar Evolution and Nucleosynthesis, Mc Graw–Hill
Cox, A.N., Kidman, P.B. 1984, Theoretical Problems in Stellar Stability and Oscillations, Proceedings of the 25th Liege International Astrophysical Colloquium, p. 259
Davis, R. Jr. 1993, Frontiers of Neutrino Astrophysics, Suzuki Y. and Nakamura K. (eds.), Universal Acad. Press Inc., Tokyo, Japan, p. 47
Davis R. 1994, Prog. Part. Nucl. Phys., Faesllor A. (ed.), Pergamon Press, 32, 13
De Boor C. 1978, A Practical Guide to Splines Springer; third ed. 1985
Duvall Jr. T.L., Harvey J.W. 1984, Nature 310, 19
Dzitko, H., Turck-Chieze, S., Delbourgo-Salvador, P., Lagrange, C. 1995, ApJ 447, 428
Eggleton, P., Faulkner, J., Flannery, B. 1973, A&A 23, 325
Endal, A.S., Sofia, S. 1978, ApJ 220, 279
Garcia-Lopez, R.J., Spruit, H. 1991, ApJ 337, 268
Gavryuseva, E., Gavryusev, V. 1994, A&A 286, 305
Henyey, L., Vardya, M., Bodenheimer, P. 1965, ApJ 142, 841
Hirata, K.S., Inoue, K., Kajita, T., Kihara, K., Nakahata, M., Nakamura, K., Ohara, S., Sato, N., Suzuki, Y., Totsuka, Y., Yaginuma, Y., Mori, M., Ohyama, Y., Suzuki, A., Takahashi, K., Yamada, M., Koshiba, M., Nishijima, K., Suda, T., Tajima, T., Miyano, K., Miyata, H., Takei, H., Fukuda, Y., Kodera, E., Nagashima, Y., Takita, M., Kaneyuki, K., Tanimori, T., Beier, E.W., Feldscher, L.R., Frank, E.D., Frati, W., Kim, S.B., Mann, A.K., Newcomer, F.M., van Berg, R., Zhang, W. 1991, Phys. Rev. Lett., 66, 9
Hulburt, N.E. Toomre, J. Massaguer, J. M. 1986, ApJ, 311, 536
Knobloch, E. 1977, J. Fluid Mech. 83, 129
Kurucz, R.L. 1991, Stellar Atmospheres : Beyond Classical Models Crivellari L., Hubeny I. and Hummer D. (eds.), NATO ASI Series, Kluwer, Dordrecht 1991
Lebreton, Y., Maeder, A. 1987, A&A 175, 99
Marchouk, G., Agochkov, V. 1985, Méthode des Eléments Finis, Mir
Michaud, G., Proffitt, C.R. 1991, IAU Colloq. 137, Inside the Stars, ed. A. Baglin & W.W. Weiss (San Francisco: ASP), 246
Montalban, J. 1994, A&A 281, 421
Montalban, J. 1995, A&A (in press)
Morel, P. 1989, Un code d'Evolution Stellaire Adaptatif et Modulaire, Cours de Structure Interne, Ecole d'Aussois, Hubert A.M. and Schatzman E. (eds.), Publ. Obs. Paris
Morel, P. 1993, Inside the Stars, IAU colloquium 137, ASP Conf. Ser., 40, Weiss W.W. and Baglin A. (eds.), p. 445
Morel, P. 1995, Cours de Structure Interne, Ecole d'Aussois, Schatzman E. (ed.), Publ. Obs. Paris, p. V-1
Pinsonneault, M.H., Kawaler, S.D., Sofia S., Demarque P. 1989, ApJ 338, 424
Press, W.H. 1981, ApJ 245, 286
Press, W.H., Ribicky, G.B. 1991, ApJ 248, 751
Michaud, G. Proffitt, C.R. 1991, ApJ 380, 238
Provost, J. 1984, Observationnal Tests of the Stellar Evolution Theory, IAU Symposium 105, Maeder A. and Renzini R. (eds.), D. Reidel Publishing Company, p. 47
Provost, J. 1995, private communication
Quarteroni, A., Valli, A. 1994, Numerical Approximation of Partial Differential Equations, Springer Verlag
Richer, J., Michaud, G. 1993, ApJ 416, 312
Rieutord, M., Zahn, J.P. 1995, A&A 296, 127
Rogers, F., Iglesias, C. 1992, ApJS 79, 507
Schatzman, E. 1969, A&A 3, 331
Schatzman, E. 1970, Physics and Astrophysics, Lectures delivered at CERN, 1970, Published by CERN
Schatzman, E., Maeder, A. 1981, Nature 290, 683
Schatzman, E., Maeder, A., Angrand, F., Glowinski, R. 1981, A&A 96, 1
Schatzman, E. 1991, Mem. Soc. Astron. Ital. 62, 111
Schatzman, E. 1991, Angular momentum evolution of young stars, NATO Advanced Research Workshop on Angular momentum Evolution of Young Stars, Noto (Italy), Catalano S. and Stauffer J.R. (eds.), p. 223
Schatzman, E. 1991, Solar Interior and atmosphere, Cox A.N., Livinston W.C., Matthews M.S. (eds.), Space Sci. Ser., University of Arizona Press, Tucson, AZ, p. 192
Schatzman, E., Baglin, A. 1991, A&A 249, 125
Schatzman E. 1993, A&A 279, 431
Schatzman, E. 1994, Colloquium of Seattle (in press)
Schatzman, E., Montalban, J. 1995, Physical Processes in Astrophysics, Masnou J.L. (ed.), Springer, (in press)
Schumaker, L. 1981, Splines Functions : Basic Theory, John Whiley
Steffen, M., Freytag B. 1991, Reviews of Modern Astronomy, 4, Klare G. (ed.), Springer-Heidelberg, p. 43
Steffen, M. 1993, Inside the Stars, IAU colloquium 137, ASP Conf. Ser., 40, Weiss W.W. and Baglin A. (eds.), p. 300
Toutain, Th., Frölich, C. 1992, A&A 257, 287
Turck-Chièze, S., Däppen, W., Fossat, E., Provost, J., Schatzman, E., Vignaud, D. 1993, Physics Reports, The Solar Interior, 230, 59
Zahn, J.P. 1983, Astrophysical Processes in upper Main Sequence Stars, Hauck B. and Maeder A. (eds.), Geneva Observ.
Zahn, J.P. 1990, Inside the Sun, IAU Colloquium NA1121, Berthomieu G., Cribier M. (eds.), Kluwer Academic Publishers, p. 425

This article was processed by the author using Springer-Verlag LaTeX A&A style file *L-AA* version 3.